

# DEPLOYMENT STUDY OF A SELF-RIGIDIZABLE INFLATABLE BOOM

Houfei Fang and Michael Lou  
Jet Propulsion Laboratory  
California Institute of Technology  
Pasadena, California

John Hah  
Hah Hah & Associates, Inc.  
Monterey Park, California

## Abstract

Deployment dynamic behavior of an inflatable space structure is analyzed using a combination of gas dynamic analysis and rigid body kinematics simulations. Modeling technique is presented for deployment of a simple cantilever boom that is rolled up on a cylindrical mandrel. During this deployment process, boom vibration is captured with the analytical models. The deployment process of a five-meter inflatable/self-rigidizable boom has also been tested and the test results correlated very well with analytical simulations.

## 1. Introduction

During the past several years, JPL has been developing a new class of self-rigidizable space inflatable structures, identified as the Spring-Tape-Reinforced (STR) aluminum laminate booms, or simply STR booms<sup>1, 2</sup>. These STR booms have been used as the primary inflatable structural elements for several large, space-deployable radar antennas, including a Ka-band reflectarray antenna<sup>3</sup> and a L-band synthetic aperture radar<sup>4</sup>. The basic construction of the boom consists of an aluminum laminate tube and four spring tapes attached to the inside wall of the tube in the axial direction<sup>5</sup>. At this time, commercially available stainless steel measuring tapes, commonly known as the carpenter tapes, are used. However, for future space flight

applications, we plan to use reinforcement tapes that are made of more advanced materials, such as titanium or composites.

With a wall thickness less than 0.1 mm, a STR boom can be easily deflated, flattened, and rolled-up (or folded-up) for stowage. During the process of flattening and stowing a STR boom, strain energy is stored in the rolled-up (or fold-up) tapes. To avoid any unintentional self-deployment of the stowed boom, as well as to control the deployment dynamics during its in-space deployment, some form of deployment control must be implemented. This has been accomplished for most of the STR booms used in inflatable antennas by attaching Velcro strips to the outside surface of the boom. These Velcro strips will hold the stowed boom to prevent pre-mature deployment and will delaminate when commanded deployment starts and a relatively low inflation pressure is fed into the boom. The deployment speed is hence controlled by the rate of pressurized air that flows into the boom and the resistive force provided by the delaminating Velcro strips<sup>6</sup>. Figures 1 are a set of sequential photos showing a controlled deployment of a 5-meter-long STR boom equipped with Velcro strips. One unique advantage of the STR boom is that it preserves a certain level of stiffness during the entire deployment process. Also, during the deployment of a STR boom, the strain energy stored in the rolled-up or folded-up tapes is being released. As a result, the boom can potentially undergo vibration motions during the deployment. In the extreme cases, very violent deployment could happen if the deployment-control system, such as that using the Velcro strips, would fail. To address this issue, a study on the deployment dynamics of long STR booms that is rolled-up on a mandrel has been initiated.

---

Copyright © 2002 by the American Institute of Aeronautics and Astronautics, Inc. The U.S. Government has a royalty-free license to exercise all rights under the copyright claimed herein for governmental purpose. All other rights are reserved by the copyright owner.

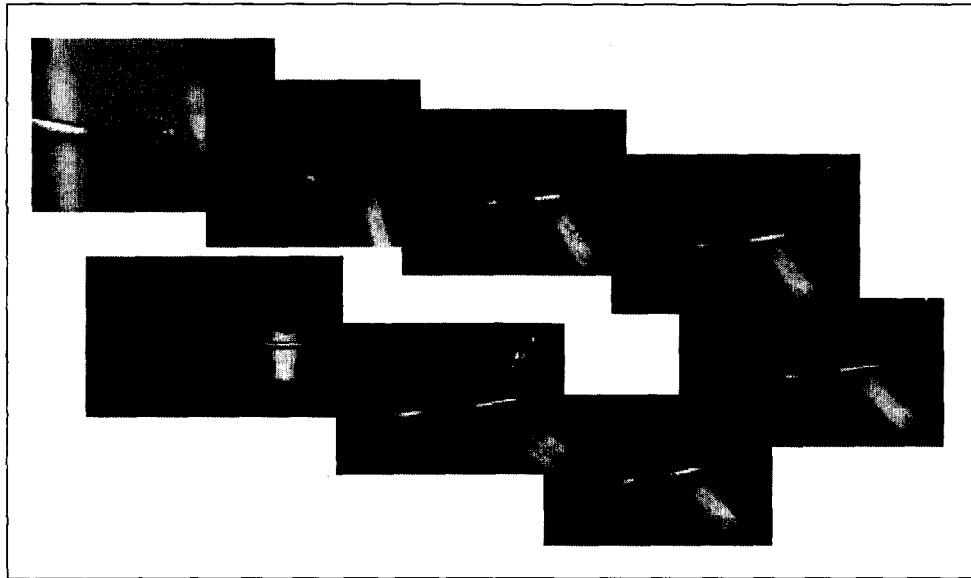


Figure 1. Inflation deployment of a 5-meter STR boom

Deployment tests and analyses of inflatable booms have been extensively conducted previously. Clem and his associates conducted deployment tests of inflatable booms<sup>7</sup>. Campbell and her coworkers experimentally investigated the effects of gravity to the deployment of inflatable tubes<sup>8</sup>. Fay and Steele derived equations of forces for large deformation of an inflated cylindrical tube<sup>9</sup> and Tsoi used these equations to simulate the deployments of fold-up and rolled-up booms<sup>10</sup>. Haug and colleagues employed finite element method to simulate the deployment process of an inflatable antenna<sup>11</sup>. Miyazaki and Uchiki tested and analyzed the inflation deployment of a one-fold boom<sup>12</sup>. Wang and Johnson used LS-DYNA to analyze the deployment of a Z-fold tube<sup>13</sup>. However, all these previous studies focused on the pressure-stabilized inflatable booms, which means pressure has to be kept inside the booms to maintain the rigidity of the booms. Deployment dynamics of relatively long (several meters to several tens of meters) and instantly rigidizable booms (stiffness does not depend on the pressure), such as the STR booms, has not been investigated before. The deployment process of an instantly rigidizable boom involves varying stiffness, varying mass distribution, and varying resonant frequencies. For this type of booms, lateral vibrations are introduced by deployment processes and will be investigated by this study.

The methodology of analytically modeling and simulating the deployment dynamics of instantly rigidizable booms is composed of three major steps. Details of these steps will be discussed in the following section. Deployment tests and analyses of a five-meter STR Aluminum Laminate boom will be presented subsequently. Some physical phenomena observed by this study will also be discussed.

## 2. An analytical Model of the Deployment Analysis

The inflatable boom being analyzed is initially flattened and rolled-up on a mandrel (the boom can also be z-folded). The first step is to discretize the boom into a large, but finite, number of compartments along the axial direction of the boom. The second step of this analysis is to calculate, based on gas dynamic theory, the pressure and volume variations of each compartment as functions of time. The original volume of each compartment is assumed to be zero and the original pressure is set equal to the ambient pressure. The volume, pressure, mass, and temperature of each compartment can be described by a group of differential equations. The volume and pressure change as functions of time of every compartment are thus obtained by integrating these equations. These results are used to determine the timing of each compartment as it starts to deploy and the duration required to finish the deployment.

The third step is the implementation of a structural/kinematic model for simulating the dynamic behavior of the boom during the deployment process. In this step, each compartment is represented by a rigid beam element. A torsional spring and damper system is used to connect two adjacent elements. The mass distributions of this model are identical to the deployed boom. The stiffness is tuned to match closely to the structural behavior. The strain energy of the torsional springs is sequentially released based on the timing determined from the previous step of gas dynamic analysis to characterize the deployment process. With accurate mass and stiffness distributions of the boom and the mandrel, this method is able to predict the deployment dynamics in a fairly accurate manner. Details of step two and step three of the method are described below.

## 2.1. Step Two—Gas Dynamic Analysis

It is assumed that the gas used to inflate the boom behaves as an ideal gas with constant specific heat and that there is no heat transfer into the control volume (adiabatic). It is further assumed that the temperature and pressure of the gas are uniform within the control volume of an individual boom compartment. As a result,

$$P_i V_i = m_i R T_i \quad (1)$$

is valid for each compartment. In equation one,  $P_i$ ,  $V_i$ ,  $m_i$  and  $T_i$  denote pressure, volume, mass, and temperature of the  $i^{\text{th}}$  compartment and  $R$  is the gas constant.

The rate of mass changing of the  $i^{\text{th}}$  compartment at time  $t$  is determined by the flow rates of its boundaries,

$$\frac{dm_i}{dt} = \dot{m}_{in} - \dot{m}_{out} = \dot{m}_{hi} - \dot{m}_{ij} \quad (2)$$

where subscript  $i$  denotes the current compartment,  $h$  denotes the previous compartment, and  $j$  denotes the next compartment.  $\dot{m}_{in}$  is the mass rate of gas flowing into the  $i^{\text{th}}$  compartment from  $h^{\text{th}}$  compartment and  $\dot{m}_{out}$  is the mass rate of gas flowing out from the  $i^{\text{th}}$  compartment to  $j^{\text{th}}$  compartment.

The mass flow rate from one compartment to the next compartment is approximated by one-

dimensional, quasi-steady, isentropic flow and formulated as<sup>14</sup>,

$$\frac{dm_{ij}}{dt} = A_{ij} \frac{P_i}{R\sqrt{T_i}} \left(\frac{P_e}{P_i}\right)^{\frac{1}{k}} \sqrt{2g \left(\frac{kR}{k-1}\right) \left(1 - \left(\frac{P_e}{P_i}\right)^{\frac{k-1}{k}}\right)} \quad (3)$$

where  $k = c_p / c_v$  is the specific heat ratio of the gas,  $P_e$  is the exhaust pressure between two compartments,  $A_{ij}$  is the connecting area between two compartments and  $j = i + 1$ . The critical pressure  $P_c$  at which sonic flow occurs can be calculated by,

$$\frac{P_c}{P_i} = \left(\frac{2}{k+1}\right)^{\frac{k}{k-1}} \quad (4)$$

The pressure  $P_e$  in equation 3 is given by,

$$P_e = P_j \quad \text{while } P_j > P_c$$

or

$$P_e = P_c \quad \text{while } P_j < P_c.$$

The connecting area between compartment  $i$  and compartment  $j$  can be defined by,

$$A_{ij} = \begin{cases} 0 & V_i < \frac{a_i}{b_i} V_i^* \\ \left(\frac{b_i \frac{V_i}{V_i^*} - a_i}{b_i - a_i}\right) A & V_i \geq \frac{a_i}{b_i} V_i^* \end{cases}, \quad (5)$$

where  $V_i^*$  is the fully inflated volume of the  $i^{\text{th}}$  compartment and  $A$  is the cross-sectional area after the compartment is fully inflated. This equation represents the fact that the

compartment  $j$  stays deflated until  $\frac{a_i}{b_i} \times 100\%$  of

the previous compartment, compartment  $i$ , has been filled.  $a_i$  and  $b_i$  depend on the deployment control system (e.g. peel strength of the Velcro strips) and can be determined by experiment.

The state (pressure, volume, temperature, and mass) of each compartment can be determined by the first law of thermodynamics. For an adiabatic process,

$$\frac{d}{dt} (m_j c_v T_j) = c_p T_i \dot{m}_{in} - c_p T_j \dot{m}_{out} - P_j \frac{dV_j}{dt}, \quad (6)$$

where  $c_v$  and  $c_p$  are the specific heat of the gas with constant volume and pressure, and  $j=i+1$ . On the other hand,

$$\frac{d}{dt}(m_j c_v T_j) = m_j c_v \frac{dT_j}{dt} + c_v T_j \frac{dm_j}{dt}. \quad (7)$$

Combining equations (6) and (7) with (1) yields,

$$\frac{\dot{T}_j}{T_j} = \frac{1}{m_j}(\dot{m}_{out} - \dot{m}_{in}) + \frac{k}{m_j} \left( \frac{T_i}{T_j} \dot{m}_{in} - \dot{m}_{out} \right) - \frac{(k-1)}{V_j} \dot{V}_j \quad (8)$$

The pressure of compartment  $j$  is defined by

$$P_j = P_a + (P_i - P_a) \frac{V_j}{V_j^*}, \quad (9)$$

where  $P_a$  is the environmental pressure and  $V_j^*$  is the fully deployed volume of the  $j^{\text{th}}$  compartment. Equation (9) means that, the pressure of  $j^{\text{th}}$  compartment equals to the environmental pressure before it starts to deploy and equals to the pressure of the previous compartment after it is fully deployed. The derivative of equation (9) is,

$$\dot{P}_j = \dot{P}_i \frac{V_j}{V_j^*} + (P_i - P_a) \frac{\dot{V}_j}{V_j^*} \quad (10)$$

For every compartment, a group of differential governing equations can be obtained from equations (1), (2), (5), (8), (10) and expressed as,

$$\begin{bmatrix} 0 & 0 & 0 & 0 & m_j V_j & V_j T_j & 0 & (k-1)m_j T_j \\ 0 & 0 & 0 & 0 & 0 & 1 & 0 & 0 \\ 0 & 0 & 0 & 0 & -m_j R & -RT_j & V_j & P_j \\ 0 & 0 & V_j & 0 & 0 & 0 & -V_j^* & (P_i - P_a) \end{bmatrix} \begin{Bmatrix} \dot{T}_i \\ \dot{m}_i \\ \dot{P}_i \\ \dot{V}_i \\ \dot{T}_j \\ \dot{m}_j \\ \dot{P}_j \\ \dot{V}_j \end{Bmatrix}$$

$$= \begin{Bmatrix} 0 \\ 0 \\ 0 \\ 0 \\ kT_i V_j \dot{m}_{in} - kT_j V_j \dot{m}_{out} \\ \dot{m}_{in} - \dot{m}_{out} \\ 0 \\ 0 \end{Bmatrix} \quad (11)$$

In equation (11),  $\dot{m}_{in}$  and  $\dot{m}_{out}$  can be calculated by equation (3) and  $j=i+1$ . Governing equations of all compartments are systematically assembled to form a group of

governing equations to represent the whole boom. The state of each compartment is then calculated by integrating this group of differential equations with respect to time. Runge-Kutta method has been used by this study to numerically integrate this group of differential equations. As a result, pressure and volume as functions of time of each compartment are calculated. The time at which when a compartment starts to deploy, as well as when a compartment finishes the deployment and becomes fully inflated, can thus be determined from the pressure and volume of that compartment. The third step of the deployment analysis can then be started with the timing information obtained from this step of gas dynamic analysis.

## 2.2. Step Three—Structural Dynamic Analysis

The final step of this analysis is to create a structural/kinematic model that can be used to simulate the dynamic behavior of the deploying boom. The approach to create such a model starts with the assumption that the structural behavior of a cantilever boom can be reasonably modeled as a series of rigid links that are hinged together by torsional springs. By controlling the torsional stiffness, the bending behavior of a cantilever boom can be closely modeled by rigid body dynamics of these links. The purpose of the hinge is to provide kinematic constraints for these rigid links to allow only appropriate movements similar to bending behavior. The torsional springs control the bending stiffness of the cantilever boom yield the proper natural frequencies. Other components such as dampers and external torsional forces are also added to the model to aid in simulating the desired deployment process.

The simulation model starts with the boom in its initial deflated and rolled up state. A cylindrical mandrel is attached to the free end of the cantilever boom with the appropriate mass representation that includes not only the actual mandrel, but also the end cap. The driving mechanism for the mandrel to un-roll comes from the strain energy of the torsional springs. The magnitude of this strain energy is determined by the spring stiffness and the required rotation to wrap the straight boom around the circular mandrel. In the simulated deployment process, the strain energy from the torsional springs must be released in a sequential order in accordance with the timing

required to inflate the boom. To achieve this, an applied torsional force with magnitude equal to the strain energy of the spring is applied on top of the individual torsional springs. The sequential removal of this torsional force, with timing derived from the gas dynamic analysis, activates and releases the strain energy of the spring in a similarly sequential manner to deploy the boom.

The stiffness of each torsional spring is initially derived based on the moment rotation relationship of a cantilever boom under both a tip loading and distributed loading conditions. The mass of the system remains constant based on the physical property of the boom and the mandrel. Damping is assumed to be negligible during tuning. By observing the natural vibration of the boom after the deployment, the stiffness of the torsional springs can be numerically tuned to match the physical or theoretical values.

### 3. A Case Study

The boom modeled and tested in this study is a five-meter long STR boom. The cross-section of the STR boom has been shown in Figure 1 and the diameter of the boom is 7.62 cm. The aluminum laminate of the boom is composed of 0.0254-mm Polyester—0.0762-mm soft aluminum—0.0254-mm Polyester. The total weight of the boom is 1.28 kg, including the Velcro. The boom is rolled-up on a 0.165-m diameter mandrel as shown in Figure 2 and the weight of the mandrel (includes the end-cap) is 0.56 kg. The bending stiffness of the boom ( $EI$ , the product of modulus of elasticity and moment of inertia) in its deployed state is experimentally determined<sup>5</sup> to be  $2061 \text{ Nm}^2$ .



Figure 2. A 5-m STR boom rolled up on a 0.165-m diameter mandrel

#### 3.1 Tests

A six-meter long rectangular test frame was constructed to conduct tests on the STR boom under study. Figure 3 is the picture of the frame. This frame was assembled by using Bosh extrusion beams and two ½" aluminum plates. One of the test boom's end caps was used to attach the boom to the upper aluminum plate of the test fixture as shown in Figure 4.



Figure 3. Test frame

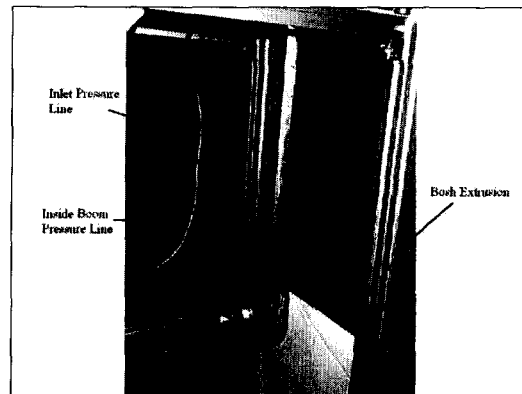


Figure 4. Test setup

Two video cameras were used to record test results. Camera 1 was set to record the pressure fluctuations and camera 2 was set to record the movement at the center of the mandrel during deployment. In order to record the movement at the center of the mandrel, a laser beam was attached to the center of the mandrel as seen in Figure 5. The light beam projected onto a sheet of paper with dimensional markings. Camera 2 followed the projected light beam throughout the deployment recording the horizontal and vertical movements of the light beam.

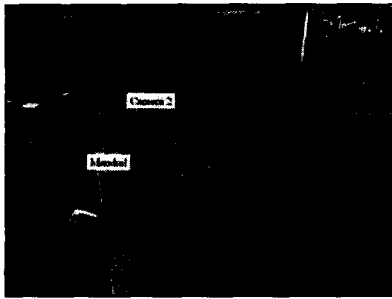


Figure 5. Light beam setup

In Figure 4, two air hoses are distinctly identified. One of the lines is connected to a digital pressure gauge reading the inlet pressure used to deploy the boom. The second line is connected to another digital pressure gauge that reads the pressure inside the boom. The pressure readings from the video camera were tabulated into a spreadsheet. Figure 6 is a graphical result of the inlet and internal pressure of the boom with respect to time. The initial inlet deployment pressure was set to 23.6 KPa.

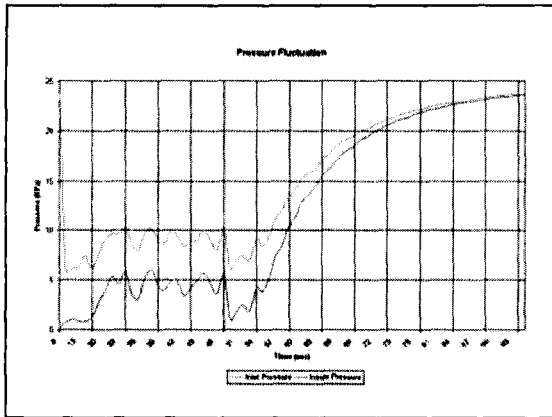


Figure 6. Graphical results of pressure fluctuations

The recorded data from camera 2 was also inputted into a spreadsheet program. The lateral displacement of the mandrel with respect to time was plotted as shown in Figure 7. A second test was run using an inlet pressure of 25.2 KPa. The graphical results between the second test and the one shown in Figure 7 correlated very well.

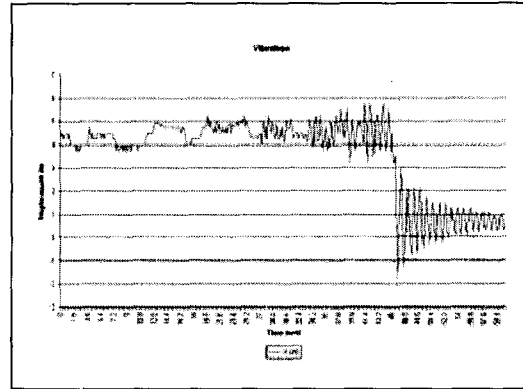


Figure 7. Vibration of the mandrel during the boom deployment

### 3.2. Analyses

The 5-m long boom is first partitioned into 74 compartments. Based on the gas dynamic analysis procedure described in section 2.1, pressure and volume of each compartment were calculated. Figure 8 shows the volumes variation of the first eight compartments with respect to time. The deployment timing of each rigid-link element, i.e. the timing when a compartment starts to deploy and when a compartment finishes the deployment, can thus be determined based on the volume variation of that compartment.

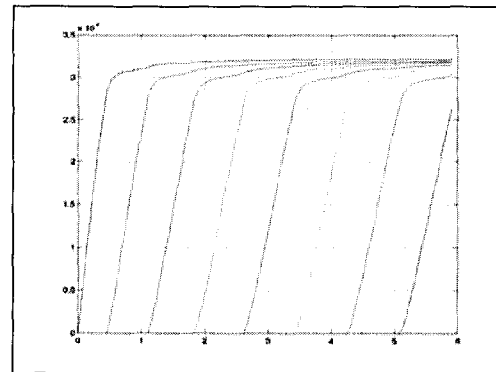


Figure 8. Volumes of the first eight compartments as functions of time

After the gas dynamic analysis, a structural/kinematic analysis model is created to simulate the deployment process of the 5-m STR boom. In this model, the 5-m boom is again divided into 74 individual rigid links. The mandrel and the end caps are also modeled as a cylinder with the appropriate dimension that matches the physical size. The mass of the 5-m

boom is measured to be about 1.28 Kg and this mass is evenly distributed to the 74 rigid links at 0.17 Kg each. The mass of the mandrel and one end cap of the boom is measured to be 0.56 kg and this mass is used in the model as the tip mass of the cantilever beam. In this model, the 5-m boom is wrapped around the mandrel in approximately 9 revolutions. Therefore, each revolution of the boom consists of 8 rigid links and each link rotates about 45 degree to conform to the circumference of the mandrel. The structural/kinematic model with the boom partially deployed is shown in Figure 9.

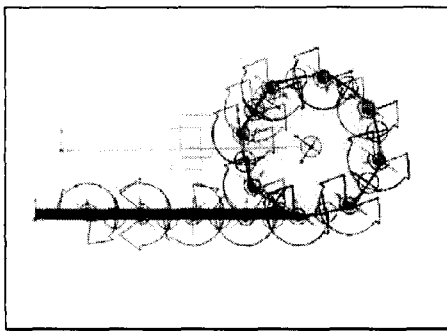


Figure 9. Structural/kinematic model of a deploying boom

The analytical results are plotted on top of the test result as shown in Figure 10 for easy comparison. Figure 11 focuses on the lateral vibration during the final 5 seconds of deployment and the subsequent free vibration phase of the boom. The analytical model matched well during the deployment process as well as after the boom is fully deployed. It is observed from both test and analytical results that the vibration magnitude significantly increased during the last several seconds of deployment. The vibration is then slowly damped out after the boom is fully deployed.

The vibration observed during the first 2/3 of the span is to be ignored as it is due to numerical noise from the length of the rigid link. With only 8 links per revolution and each link must go thru 45 degrees of rotation during the deployment, the large angle of rotation has caused the noisy movements observed in the analytical results. The magnitude of this numerical noise is reducible with a refined model composed of larger number of rigid links.

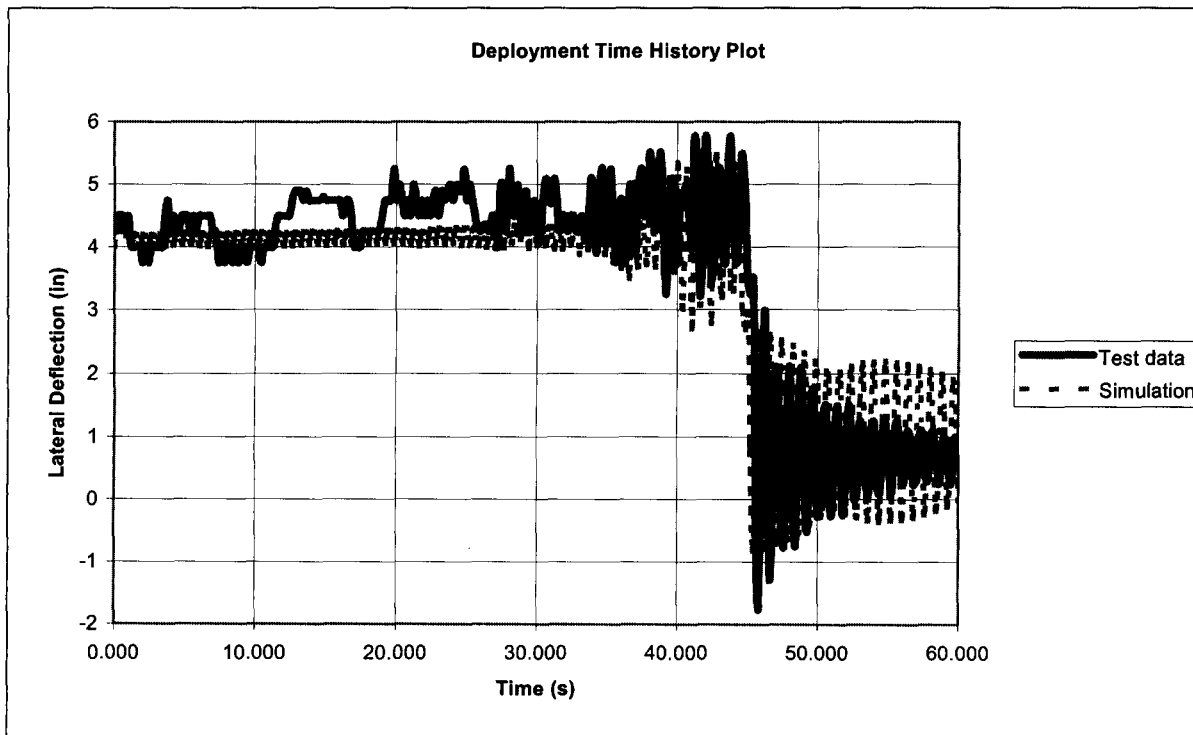


Figure 10. Comparison of mandrel vibration during deployment

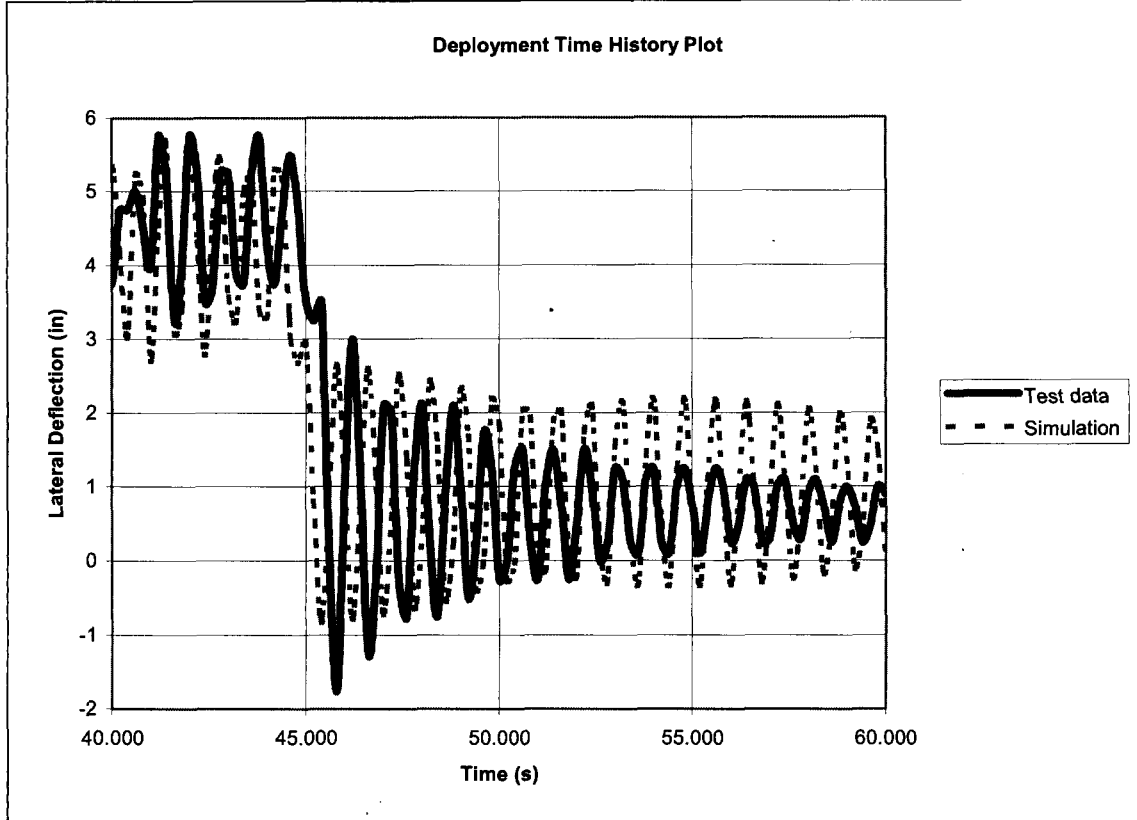


Figure 11. Comparison of mandrel vibration during the final 5 seconds and free vibration phase

#### 4. Concluding Remarks

The current method adjusts the stiffness of the torsional springs based on numerical tuning of the analytical natural frequency with theoretical or test value. A better method of determining the spring stiffness for structural/kinematic modeling needs to be developed in the future.

The damping of the analytical model is controlled by the torsional damper at the hinge. The amount of damping is tuned based on the exponential decay observed from the physical test. After the boom is fully deployed, the natural vibration and the decay of amplitude can be used to calculate the system damping for the simulation. Based on this approach, the simulation data matched well with physical data during deployment as well as natural vibrating phase after the deployment.

It is observed from both the physical test data and the simulation results that the magnitude of boom tip vibration does not increase significantly

in amplitude until the final 1/3 of the deployment time span. This may be attributed to the resonance effect of the system's natural frequency with the rolling speed of the mandrel. Further research should be performed to examine this phenomenon as it could play a significant role for future design and applications of very long and slim booms.

For large inflatable space structures, physical testing of long booms in weightless environment is difficult and, in some cases, not always possible. Analytical simulation of the deployment can be an effective and efficient way to assess in-space deployment of these booms prior to actual space mission. It is hoped that the study effort presented herein has contributed to the continuous development of such an important simulation tool.

#### 5. Acknowledgements

The authors wish to thank Mr. Ubaldo Quijano of California State University at Los Angeles for his

help on the tests and analyses of the boom deployments.

The work described in this paper was performed at the Jet Propulsion Laboratory, California Institute of Technology under contract with the National Aeronautics and Space Administration of United States.

## 6. REFERENCES

- [1] Fang, H. and Lou, M., "Tape-Spring Reinforcements for Inflatable Structural Tubes", NPO-20615, NASA Tech Briefs, Vol 24, No. 7, July 2000.
- [2] Lou, M., Fang, H., and Hsia, L., "A Combined Analytical and Experimental Study on Space Inflatable Booms", presented at the 2000 IEEE Aerospace Conference. Big Sky, Montana, March 2000.
- [3] Fang, H., Lou, M., Huang, J., Hsia, L., and Kerdanyan, G., "An Inflatable/Rigidizable Ka-Band Reflectarray Antenna", AIAA 2002-1706, 43<sup>rd</sup> AIAA/ASME/ASCE/ AHS/ASC Structures, Structural Dynamics, and Materials Conference and Exhibit, Denver, Colorado, 22-25 April 2002
- [4] Lopez, B., Lou, M., Huang, J., Edelstein, W., "Development of an Inflatable SAR Engineering Model", AIAA 2001-1618, presented at 42<sup>nd</sup> AIAA/ASME/ASCE/AHS/ASC Structures, Structural Dynamics, and Materials Conference and Exhibit, Seattle, WA, 16-19 April 2001
- [5] Lou, M., Fang, H., and Hsia, L., "Self-Rigidizable Space Inflatable Boom", AIAA Journal of Spacecraft and Rockets, Vol. 39, No. 5, pp.682-690
- [6] Salama, M., Fang, H., and Lou, M., "Resistive Control of Deployment of Inflatables: Analysis and Experimental Verification", AIAA 2001-1339, presented at 42<sup>nd</sup> AIAA/ASME/ASCE/AHS/ASC Structures, Structural Dynamics, and Materials Conference and Exhibit, Seattle, WA, 16-19 April 2001
- [7] Clem, A.L., Smith, S.W., Main, J.A., "Experimental Results Regarding the Inflation of Unfolding Cylindrical Tubes", AIAA 2001-1264, 42<sup>nd</sup> AIAA/ASME/ASCE/ AHS/ASC Structures, Structural Dynamics, and Materials Conference and Exhibit, Seattle, WA, 16-19 April 2001
- [8] Campbell, J. E., Smith, S. W., Main, J. A., Kearns, J., "Staged Microgravity Deployment of a Pressurizing Scale Model Spacecraft", AIAA 2002-1455, 43<sup>rd</sup> AIAA/ASME/ASCE/ AHS/ASC Structures, Structural Dynamics, and Materials Conference and Exhibit, Denver, Colorado, 22-25 April 2002
- [9] Fay, J. P., Steele, C. R., "Bending and Symmetric Pinching of Pressurized Tubes," IUTAM-IASS Symposium on Deployable Structures: Theory and Applications, Cambridge, U.K., September 1998
- [10] Tsoi, S. H. H., "Modeling and Simulation of Inflatable Space Structures," Engineer Degree Thesis, Department of Aeronautics and Astronautics, Stanford University, June 1997
- [11] Haug, E., Protard, J. B., Milcent, G., Herren, A., Brunner, O., "The Numerical Simulations of the Inflation Process of Space Rigidized Antenna structures," Proceeding of the International Conference on Spacecraft Structures and Mechanical Testing, Noordwijk, The Netherlands, April 1991
- [12] Miyazaki, Y., and Uchiki, M., "Deployment Dynamics of Inflatable Tube", AIAA 2002-1254, 43<sup>rd</sup> AIAA/ASME/ASCE/ AHS/ASC Structures, Structural Dynamics, and Materials Conference and Exhibit, Denver, Colorado, 22-25 April 2002
- [13] Wang, J. T., Johnson, A. R., "Deployment Simulation of Ultra-Lightweight Inflatable Structures", AIAA 2002-1261, 43<sup>rd</sup> AIAA/ASME/ASCE/ AHS/ASC Structures, Structural Dynamics, and Materials Conference and Exhibit, Denver, Colorado, 22-25 April 2002
- [14] Salama, M., Kuo, C., Lou, M., "Simulation of Deployment Dynamics of Inflatable Structures", AIAA Journal, Vol.38, No.12, 2000, pp. 2277-2283